The Journal of Chemical Physics

RESEARCH ARTICLE | OCTOBER 03 2023

The Debye's model for the dielectric relaxation of liquid water and the role of cross-dipolar correlations. A MD-simulations study

Fernando Alvarez ; Arantxa Arbe ; Juan Colmenero

J. Chem. Phys. 159, 134505 (2023)
https://doi.org/10.1063/5.0168588

The Journal of Chemical Physics ARTICLE pubs.aip.org/aip/jcp

The Debye's model for the dielectric relaxation of liquid water and the role of cross-dipolar correlations. A MD-simulations study

Cite as: J. Chem. Phys. 159, 134505 (2023); doi: 10.1063/5.0168588
Submitted: 19 July 2023 • Accepted: 18 September 2023 •
Published Online: 3 October 2023

Fernando Alvarez,[1,2] Arantxa Arbe,[2] and Juan Colmenero[1,2,3,a)]

AFFILIATIONS

[1] Departamento de Polímeros y Materiales Avanzados: Física, Química y Tecnología (UPV/EHU), Apartado 1072, E-20080 San Sebastián, Spain
[2] Centro de Física de Materiales (CFM) (CSIC-UPV/EHU) - Materials Physics Center (MPC), Paseo Manuel de Lardizabal 5, 20018 San Sebastián, Spain
[3] Donostia International Physics Center, Paseo Manuel de Lardizabal 4, 20018 San Sebastián, Spain

[a)] **Author to whom correspondence should be addressed:** juan.colmenero@ehu.eus

ABSTRACT

By means of massive (more than $1.2 \cdot 10^6$ molecules) molecular dynamics simulations at 300 K we have disentangled self- and cross-dipolar contributions to the dielectric relaxation of liquid water that cannot be experimentally resolved. We have demonstrated that cross dipolar correlations are of paramount importance. They amount for almost a 60% of the total dielectric amplitude. The corresponding relaxation function is a one-step Debye-like function with a characteristic time, τ_{cross}, of the order of the phenomenological Debye time, τ_D. In contrast, the relaxation function corresponding to the self-contribution is rather complex and contains a fast decay related to dipolar librations and a second relaxation step that can be well described by two exponentials: a low-amplitude fast process (τ_0 = 0.31 ps) and a main slow process (τ_{self} = 5.4 ps) that fully randomizes the dipolar orientation. In addition to dipolar relaxation functions, we have also calculated scattering-like magnitudes characterizing translation and rotation of water molecules. Although these processes can be considered as "jump" processes in the short time range, at the time scale of about τ_D–τ_{cross}, at which the cross-dipolar correlations decay to zero, the observed behavior cannot be distinguished from that corresponding to uncoupled Brownian translational and rotational diffusion. We propose that this is the reason why the Debye model, which does not consider intermolecular dipolar interactions, seems to work at time $t \gtrsim \tau_D$.

I. INTRODUCTION

Nowadays there is no doubt that water is a very complex liquid that plays a prominent role in nature. In particular, water dynamics is of paramount importance to understand many biological and physicochemical processes. Due to the high dipolar strength of water, one of the most popular techniques used to investigate water dynamics in many different systems is broad band dielectric spectroscopy (BDS).[1]

Dielectric relaxation measurements in liquids and glass-forming systems are usually carried out in the frequency domain. The measured magnitude is the frequency-dependent complex dielectric permittivity, $\varepsilon^*(\omega) = \varepsilon'(\omega) - i\varepsilon''(\omega)$, which can also be expressed as:

$$\Phi^*(\omega) = \frac{\varepsilon^*(\omega) - \varepsilon_\infty}{\varepsilon_s - \varepsilon_\infty} = \int_0^\infty \left[-\frac{d\varphi(t)}{dt}\exp(-i\omega t)\right]dt \quad (1)$$

Here, ε_∞ is the high frequency limit value of the permittivity and ε_s its static value. In this expression, $\varphi(t)$ corresponds to the autocorrelation function of the total dielectric polarization, $\vec{M}(t)$, i.e., $\varphi(t) = \langle \vec{M}(0)\vec{M}(t)\rangle / \langle |\vec{M}(0)|^2 \rangle$, where the average is over an

equilibrium ensemble. By means of a phenomenological analysis of $\Phi^*(\omega)$ or $\varphi(t)$ we can obtain two types of parameters. If we are dealing with only one process: (i) a relaxation time, τ, characterizing the time scale of the dielectric relaxation process; and (ii) some shape parameters, which characterize the functional form of $\Phi^*(\omega)$ or $\varphi(t)$. The simplest case is to consider for $\varphi(t)$ a single exponential function $\varphi(t) = \exp(-t/\tau_D)$ which in the frequency domain corresponds to $\Phi^*(\omega) = 1/(1 + i\omega\tau_D)$. This set of equations is known as Debye's model and τ_D as the Debye relaxation time. Debye arrived to this simple model in 1929[2] by considering a thermal ensemble of non-interacting rigid dipoles (molecules) subjected to an applied electric field and assuming Brownian rotational motions for the dipoles once the electric field is turned off. Debye also noticed that τ_D can be expressed as $\tau_D = \xi/2k_BT$ where ξ is the rotational friction constant and k_B the Boltzmann constant. Moreover, according to Stokes law, for a spherical particle of radius a_R, rotating in a medium with viscosity η, $\xi = 8\pi\eta a_R^3$. Then, assuming spherical dipoles (molecules): $\tau_D = 4\pi\eta a_R^3/k_BT$. On the other hand, according to the Stokes-Einstein relationship, the translational self-diffusion coefficient for such molecules can be expressed as $D = k_BT/6\pi\eta a_T$ where a_T is the molecular hydrodynamic radius for translation. Then, we obtain that $D\tau_D = 2a_R^3/3a_T$. This means that for spherical dipoles (molecules) following rotational and translational isotropic diffusion, $D\tau_D \approx$ constant independently of temperature.

In the case of water, although nowadays we know that at high frequencies $\varepsilon''(\omega)$ deviates from a simple Debye-like behavior, the overwhelming contribution to $\varepsilon''(\omega)$ is a peak that can be rather well described by the Debye expression (see, e.g., Ref. 3). Accordingly, the dielectric relaxation time determined in the usual way ($\omega_{\max}\tau_D = 1$) –where $\omega_{\max}$ is the frequency corresponding to the maximum of $\varepsilon''(\omega)$ at a given temperature– is called Debye time. At 300 K $\tau_D \sim$ 8–9 ps. Interestingly enough, the values of $\tau_D(T)$ obtained from the dielectric experiments can be rather well approximated by the values obtained from the Stokes-Einstein relationship by using the water viscosity, $\eta(T)$ and a rotational hydrodynamic radius $a_R \approx 1.4$Å.[4,5] On the other hand, it has been reported[6] that the experimental values of both, $\tau_D(T)$ and $D(T)$, agree with $D\tau_D$ = constant from 255 to 305 K. Moreover, recent data[7] show that $D\tau_D = 1.92 \pm 0.05$Å^2 in a wider temperature range (270–330 K). We note, however, that if we assume that the hydrodynamic radius for rotation and translation diffusion are the same ($a_R \approx a_T \approx a$) the above value for $D\tau_D$ would imply a hydrodynamic radius $a \approx 1.7$Å. Thus, according to these results, one should be tempted to say that the Debye's model works rather well for the dielectric relaxation of liquid water. In other words, that water molecules approximately follow rotational and translational isotropic diffusion at $t \sim \tau_D$. This is the reason why, from the times of Debye, several authors have tried to construct models for the dielectric relaxation of water based on single-molecule dynamics without considering dipolar interactions (see Ref. 8 for a critical review). However, nowadays we know that in spite of the apparently simple chemical structure of a single water molecule (H_2O), liquid water is an extremely complex condensed matter system composed of networks of water molecules that are linked by hydrogen bonds (HBs), breaking and forming continuously. The structure and dynamics of such networks determine in some way the collective properties of water.[9,10]

For a dipolar system in general, $\vec{M}(t)$ can be written as $\vec{M}(t) = \sum_{i=1}^{N}\vec{\mu}_i(t)$ with $\vec{\mu}_i(t)$ the dipole moment of the i_{th} molecule and N the number of molecules in the system. Then

$$\varphi(t) = \frac{\langle \vec{M}(0)\vec{M}(t)\rangle}{\langle |\vec{M}(0)|^2\rangle} = \frac{1}{\langle |\vec{M}(0)|^2\rangle}\sum_{i=1}^{N}\langle \vec{\mu}_i(0)\vec{\mu}_i(t)\rangle + \frac{1}{\langle |\vec{M}(0)|^2\rangle}\sum_{i=1}^{N}\sum_{\substack{j=1\\ j\neq i}}^{N-1}\langle \vec{\mu}_i(0)\vec{\mu}_j(t)\rangle = \varphi_{self}(t) + \varphi_{cross}(t) \quad (2)$$

The amplitude of $\varphi_{self}(t)$ is just $\varphi_{self}(0) = 1/G_k$ where G_k is the finite system Kirkwood correlation factor defined as $G_k = \langle |\vec{M}(0)|^2\rangle/N\mu^2$. Accordingly, the amplitude of $\varphi_{cross}(t)$ is $\varphi_{cross}(0) = 1 - 1/G_k$. Because of the long-range nature of dipolar interactions, not only self-dipolar correlations, $\langle \vec{\mu}_i(0)\vec{\mu}_i(t)\rangle$, but also cross-terms, $\langle \vec{\mu}_i(0)\vec{\mu}_j(t)\rangle$, can play an important role in $\varphi(t)$ and $\Phi^*(\omega)$, in particular, for strongly polar systems.[11] The existence and possible relevance of cross-dipolar contributions is well known from the early times of dielectric spectroscopy (see, e.g., Refs. 12–14). However, due to the impossibility of experimentally separating self- and cross-dipolar terms, this separation has not usually been considered in the analysis of experimental data. In fact, the idea that cross-correlations might be negligible – or that they should decay as the self-terms do—was widely extended. Recently, the direct comparison between dielectric relaxation and depolarized light scattering data – together with the development of computational methods – has allowed revisiting this question and highlighting the relevance of cross-correlation terms in the dielectric response of polar liquids, as water, and glass-forming systems.[11,15–20] A new theory that considers dipolar interactions has also been recently proposed.[21]

In the case of water, due to the HB network, the orientational motions of different dipoles (molecules) become strongly correlated over large distances. Then, why the Debye's model, which does not consider dipole interactions, seems to work? Here we investigate this question by molecular dynamic (MD) simulations, that allow reproducing in a reasonable way the experimental results. These simulations allow not only separating self- and cross-dipolar contributions, but also following what the water molecules do during the dielectric relaxation. Even though we are dealing with dielectric relaxation, we have also adopted the point of view of a scattering "practitioner" and we have calculated—in addition to the total dielectric function $\varphi(t)$ and its self- and cross-contributions—the mean squared displacement and the intermediate scattering function of the relative motion of hydrogen atoms (positive charges) of a water molecule with respect to the center of the negative electrical charges, i.e., the individual dipolar dynamics. We have also calculated the mean squared displacement of the center of mass of water molecules. We have found that the cross-dipolar-correlations are of paramount importance for the dielectric relaxation of water. However, these correlations decay at a time close to the Debye time, τ_D. In fact, we have demonstrated that at this time range, the dynamics of water molecules cannot be distinguished from decoupled translational and orientational Brownian motions as it is considered in the Debye model.[2] This is the reason why, in spite of the complexity of

water molecular dynamics, the Debye model that does not contain dipolar interactions seems to work at $t \gtrsim \tau_D$.

II. MOLECULAR DYNAMICS (MD) SIMULATION METHODS

A. MD-simulation details

We have carried out massive MD-simulations of water by means of the free open-source GROMACS package, within the release version 2020.1. The TIP4P-EW model[22] was chosen to create a cubic box containing 1 223 871 water molecules that, after the customary equilibration and optimization procedures, yields a cubic cell length of 332.62 Å at a temperature value of 300 K. The production runs were carried out under NVT conditions (fixed number of molecules N, cell volume V, and temperature T). In order to evaluate the electrostatic-like contribution terms, the Particle Mesh Ewald algorithm was used and the standard Nose-Hoover protocol algorithms were chosen as a thermostat and a barostat. A first production run was calculated for 2.5 ns recording data every 0.1 ps, and, in order to get an even better insight into the hydrogen bonding behavior, we performed a subsequent 100 ps long MD simulation, saving data every femtosecond. In neither of them, the so-called "lincs" constraint algorithm was used to fix the hydrogen bond lengths. Data corresponding to the two different runs perfectly agree in the overlapping range. From the simulation trajectories we have calculated the dielectric magnitudes and the scattering-like magnitudes following the protocols that are described below. In spite of the limitations of the TIP4P-EW model,[22–24] we obtain a rather good agreement between $\varepsilon''(\omega)$ calculated from the simulations and experimental data from different sources.[3,25,26]

B. Computation of the dielectric relaxation function and validation

In order to calculate from the molecular dynamics simulations results different correlators of dipolar character, the following procedure was undertaken. First, for each and every water molecule its electric dipole moment was calculated assuming that the negative charge was sitting on the dummy atom of the four site TIP4P-EW model,[22] and both hydrogen atoms had positive values. If one averages the scalar product of these dipole values at different delay time values, all along the simulation, the self-dipole correlation function, $\varphi_{self}(t)$, is, thus, obtained. We note that this correlator cannot be directly measured from a dielectric spectroscopic technique. In addition, we have also calculated the autocorrelation functions, not for the separate individual molecular dipoles, but, instead, for the dipoles resulting from the addition to a single one of all other dipoles which should be closer to the chosen one than a certain reference distance, r. This is equivalent to calculating the total dipole moment for all dipoles inside a sphere of radius r centered in the chosen molecule. Of course, we made significant enough averages for the central water molecules all along the simulated box. Obviously, for r values below intermolecular distances, only one dipole is within the spheres and one gets, again, the self-dipole correlation. However, by increasing the extent of the radius value, one should expect that at certain r-value (r_c) one gets the dipole correlation function that should represent the bulk behavior and thereby mimic the experimental dipole response. This would imply that for $r \geq r_c$ the relaxation function $\varphi(t) = \langle \vec{M}(0)\vec{M}(t)\rangle / \langle |\vec{M}(0)|^2 \rangle$ [see Eq. (2)] would always be the same independently of r. It is noteworthy to say that for a single chosen molecule, although the number of molecules that contribute to the sum of the total dipole fluctuates around a constant value, only the central one is always bound to be inside the sphere, whereas the rest are free to enter, leave and/or reenter the sphere as the molecular dynamics evolves. We note that by means of this procedure, we are not only sampling our system (the sphere of radius r) at different times (ensemble average), but also different equivalent systems (spheres of the same radius) within our large cubic simulated cell.

Figure 1 shows the function $\varphi(t)$ calculated for different values of r [φ_r(t)]. This figure also includes the normalized $\varphi_{self}(t)$ [$\varphi_{self}(t)/\varphi_{self}(0)$] function [see Eq. (2)] for comparison. In fact, it corresponds to an r smaller than the intermolecular distance ($d \approx 3.3$ Å). As can be seen, for $r \geq 40$ Å, $\varphi(t)$ does not change with r. The inset of the figure also shows the amplitude of $\varphi_{self}(t)$, $\varphi_{self}(0) = 1/G_k(r)$—where $G_k(r)$ is the r-dependent Kirkwood factor defined as $G_k(r) = \langle |\vec{M}(0)|_r^2 \rangle / N_r \mu^2$. Here N_r is the average number of water molecules contained in a sphere of radius r. As can be seen in the inset of the figure, this amplitude does not depend on r for $r \geq 40$ Å. Obviously, the amplitude of $\varphi_{cross}(t)$, $\varphi_{cross}(0) = 1 - 1/G_k$, does not depend as well. Thus, the dipolar relaxation functions that are analyzed and discussed in the following are those corresponding to $r = 40$ Å. We note that these results are in line with those previously reported by Elton[8] that also needed to consider hundreds of molecules to reproduce the dielectric spectra. However, by using a mathematical procedure that involves the restriction of the translational motions of water molecules, Hölzl *et al.* recently reported that only about 70 molecules are enough to reproduce the frequency dependence of the dielectric losses of real water.[20] It is worth

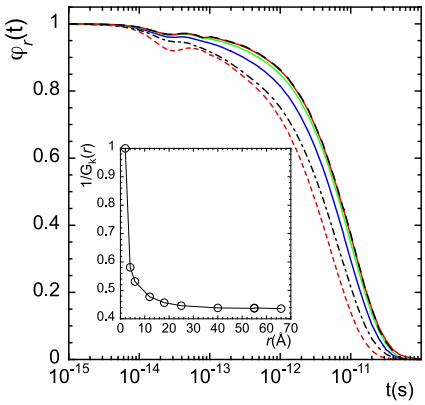

FIG. 1. Dielectric relaxation function, $\varphi(t)$, calculated for spheres with different values of the radius r: 6 Å (dashed-dot black line); 12 Å (continuous blue line); 25 Å (continuous green line); 40 Å (continuous red line); and 55 Å (dashed black line). The figure also includes the self-function, $\varphi_{self}(t)/\varphi_{self}(0)$, for comparison (dashed red line). This function in fact corresponds to $\varphi(t)$ for r smaller than the intermolecular distance. The inset shows the amplitude $[1/G_k(r)]$ of the self-contribution to $\varphi(t)$ as a function of r. It ranges from 1 at r of the order of the intermolecular distance, to a constant value of about 0.44 for $r \geq 40$ Å. The continuous line through the points is just for guiding the eye.

mentioning that in the framework of our work, the only goal of the procedure described above is to compute a reliable dipolar relaxation function—and its self- and cross-contributions—that reproduce (properly translated to the frequency domain) the experimental data.

It is worthy of remark, that the frequency dependence of the imaginary part of the dielectric permittivity, $\varepsilon''(\omega)$—calculated from the $\varphi(t)$ corresponding to $r = 40$ Å by a method based on the CONTIN program[27]—nicely agrees with experimental data from different sources[3,25,26] [see Fig. 2(a)]. Figure 2(b) shows that this agreement is particularly good in the "relaxation" frequency range, $\omega < 10^{13}$ rad/s, which is the focus of this work. Obviously, one cannot expect that the simulations with the TIP4P-EW model could reproduce perfectly the high-frequency range where polarization effects and quantum processes likely start to play a significant role.[19]

C. Computation of mean-squared-displacements and incoherent scattering functions

The scattering-like magnitudes of interest in this work are: (i) the atomic mean-squared-displacement, $\langle r^2(t)\rangle$; and (ii) the incoherent intermediate scattering function, $F(Q,t)$, where Q is the momentum transfer. In this context, "incoherent" means single particle properties. These magnitudes are mathematically related with the so-called self-part of the van Hove correlation function, $G_{self}(r,t)$, which for a particular type of atom in the sample and for an isotropic system, is defined as:[6,7]

$$G_{self}(r,t) = \frac{1}{N}\left\langle \sum_{i=1}^{N} \delta(r - |\vec{r}_i(t) - \vec{r}_i(0)|)\right\rangle \tag{3}$$

Here, $\vec{r}_i(t)$ is the position of atom i at time t, and N the number of atoms of type i. $G_{self}(r,t)$ can be computed from the atomic trajectories of the different atoms in the simulation runs, where the ensemble average is evaluated by considering different origin of times along these runs. Once $G_{self}(r,t)$ has been computed, the corresponding $\langle r^2(t)\rangle$ can be calculated as the second moment of the distribution[28,29] that for an isotropic system reads:

$$\langle r^2(t)\rangle = \int_0^\infty r^2 G_{self}(r,t) 4\pi r^2 dr \tag{4}$$

On the other hand, the intermediate scattering function, $F(Q,t)$, is defined as the Fourier transform of $G_{self}(r,t)$ to the reciprocal space,[28,29] that—again for an isotropic system—can be practically calculated as:

$$F(Q,t) = \int_0^\infty 4\pi r^2 \frac{\sin(Qr)}{Qr} G_{self}(r,t) dr \tag{5}$$

For simple cases, $G_{self}(r,t)$ is a Gaussian function expressed as:[28,29]

$$G_{self}^{Gauss}(r,t) = \left[\frac{\alpha(t)}{\pi}\right]^{3/2} \exp\left[-\alpha(t) r^2\right] \tag{6}$$

Here, $\alpha(t)$is a non-defined function of time. For instance, for a pure diffusive process, $\alpha(t) = 1/4Dt$, with D the diffusion coefficient. In the framework of the Gaussian case, $\langle r^2(t)\rangle$ is expressed as $\langle r^2(t)\rangle = 3/[2\alpha(t)]$ and $F(Q,t)$ is entirely determined by $\langle r^2(t)\rangle$ as:

$$F(Q,t) = \exp\left[-\frac{Q^2\langle r^2(t)\rangle}{6}\right] \tag{7}$$

In general, deviations from the Gaussian case can be expected. They might be quantified, in a first approximation, by the second order non-Gaussian parameter, $\alpha_2(t)$, defined as:[30]

$$\alpha_2(t) = \frac{3}{5}\frac{\langle r^4(t)\rangle}{\langle r^2(t)\rangle^2} - 1 \tag{8}$$

where $\langle r^4(t)\rangle$ is the fourth moment of the $G_{self}(r,t)$ distribution. Obviously, $\alpha_2(t)$ is zero in the Gaussian case.

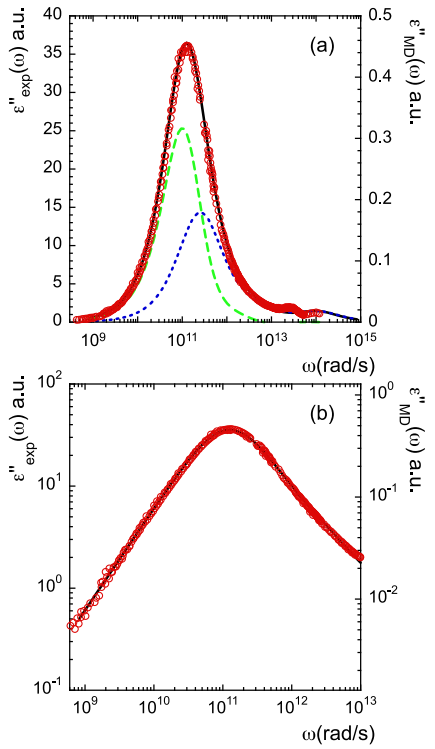

FIG. 2. (a) Comparison (linear scale) between $\varepsilon''(\omega)$, calculated from the $\varphi(t)$ corresponding to a sphere of $r = 40$ Å (continuous black line), and experimental data from different sources (red circles). A shift by a factor 1.3 has been applied to the frequency scale of the MD-simulations data. (b) The same comparison but now in a logarithmic scale and in a reduced frequency range ($\omega < 10^{13}$ rad/s). panel 2(a) also includes the self- (blue dotted line) and cross-contributions (green dashed line) to $\varepsilon''(\omega)$ calculated from the MD-simulations for comparison (see Sec. III A).

III. RESULTS AND DISCUSSION

A. Dielectric relaxation magnitudes

Figure 3 shows the dielectric relaxation results calculated from our water simulations at 300 K. The figure includes not only

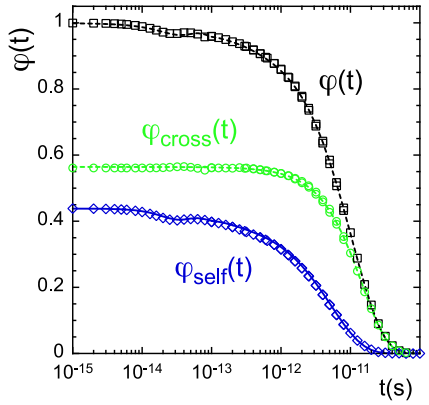

FIG. 3. Dielectric relaxation functions: $\varphi(t)$ (squares); $\varphi_{self}(t)$ (diamonds); and $\varphi_{cross}(t)$ (circles). The dashed line through the points corresponding to $\varphi_{cross}(t)$ is the fitting curve corresponding to a generalized Debye function (see the text). The dashed line through the points corresponding to $\varphi(t)$ is the total model curve (see the text). The continuous line through $\varphi_{self}(t)$ data corresponds to $\emptyset(t) = [F_{HM}(Q,t) - EISF(Q)]/[1 - EISF(Q)]$; Q is the momentum transfer (see the text, Sec. III B).

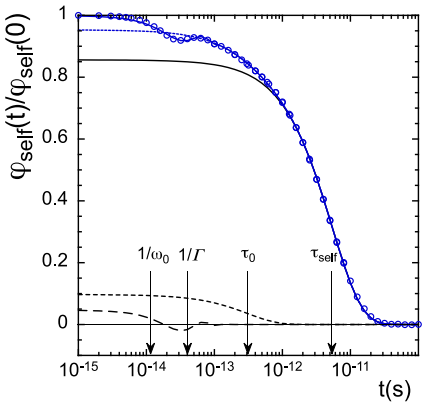

FIG. 4. Normalized self-contribution to the dipolar relaxation (blue circles). The continuous blue line through the points is the fitting curve corresponding to the proposed model [Eqs. (9)–(11)]. The other curves are the different components of the model: dipolar librations (long-dash dashed line); fast relaxation component (short-dash dashed line); slow relaxation component (black continuous line); total relaxation component (dotted blue line). The arrows mark the indicated characteristic times.

$\varphi(t) = \langle \vec{M}(0)\vec{M}(t)\rangle / \langle |\vec{M}(0)|^2 \rangle$ but also the self- and cross-terms contributions [see Eq. (2)] that, in principle, cannot be experimentally separated but are unambiguously calculated from the MD-results. We can see that the contribution of the self-term is only about 44% of the total relaxation amplitude. This highlights the paramount importance of cross dipolar correlations in the dielectric relaxation of water. From the amplitude of $\varphi_{self}(t)$, we can estimate $G_k \cong (1/0.44) = 2.3$, that is rather similar to the values recently reported[31] which were computed from MD-simulations data corresponding to different nonpolarizable and polarizable water models: SPC and SPC/E ($G_k \cong 2.5$); TIP4P ($G_k \cong 2.2$); and SWM4-DP ($G_k \cong 2.4$). This not only gives support to our results but also indicates that the amplitude of $\varphi_{self}(t)$—and thereby that of $\varphi_{cross}(t)$—seems to be very similar for different water models. The calculated self- and cross-contributions—properly transformed to the frequency domain (see Sec. II–B)—are included in Fig. 2(a) for comparison with the total $\varepsilon''(\omega)$. Qualitatively, they look-like similar to those recently reported in Ref. 19 and 20. However, we note that in those cases the authors did not quantify either the amplitude of such contributions or the equivalent value of G_k. Figure 3 shows that the short-time (high-frequency) decay of $\varphi(t)$ is mainly due to the self-contribution, because $\varphi_{cross}(t)$ is basically constant until about 0.5 ps. This regime is likely related with dipolar librations and oscillatory motions. We note that the non-vibrational decay ($t \gtrsim 0.05$ ps) of the self-contribution is not unimodal as it has been recently suggested in Ref. 20. It cannot be described by only one exponential function. A stretched exponential, or the addition of two exponentials, seems to be more appropriate. In fact, Fig. 4 shows that $\varphi_{self}(t)$ can be accurately modeled—in the full-time range—by a relaxation function, that combines two exponential functions, plus a vibrational contribution given by a damped harmonic oscillator correlation function:

$$\varphi_{self}(t)/\varphi_{self}(0) = (1 - C)\varphi_v(t) + C\varphi_R(t) \tag{9}$$

where the vibrational term is expressed as:

$$\varphi_v(t) = \exp(-\Gamma t)\cos(\omega_0 t) \tag{10}$$

and the relaxation term reads as:

$$\varphi_R(t) = (1 - A)\exp(-t/\tau_0) + A\exp(-t/\tau_{self}) \tag{11}$$

In these equations, C is the amplitude of the relaxation contribution and A that corresponding to the slow main relaxation component within the relaxation function. On the other hand, Γ and ω_0 are, respectively, the attenuation coefficient and the characteristic frequency of the damped harmonic oscillator. τ_0 and τ_{self} are the relaxation times corresponding to the two relaxation components. The values of these parameters obtained by fitting $\varphi_{self}(t)/\varphi_{self}(0)$ with Eqs. (9)–(11), are: $\Gamma = 2.49 \cdot 10^{13}$ s^{-1}; $\omega_0 = 8.70 \cdot 10^{13}$ s^{-1}; $C = 0.953$; $A = 0.898$; $\tau_0 = 0.31$ ps; $\tau_{self} = 5.4$ ps. The different contributions of the model function are included in Fig. 4. The characteristic times of the model are also indicated by arrows in this figure. We note that due to the large separation between τ_0 and τ_{self}, the model used here is basically the same that the so-called "convolution model" that has been previously used to fit both, coherent and incoherent, neutron scattering data of water[7,9] and NMR data of water as well.[32] Although this model is phenomenological, the interpretation of the fast component of the relaxation contribution is that it corresponds to "localized" motions, i.e., restricted angular motions for the dipoles. In other words, failed jump attempts, which contribution to the global dipolar reorientation is fast but limited (see the amplitude in Fig. 4). Starting from the value of $C \cdot A$ ($C \cdot A = 0.856$), i.e., the level at which $\varphi_{self}(t)/\varphi_{self}(0)$ decays by the vibration and local relaxation processes (see Fig. 4), we can have an estimation of the restricted angle explored by the dipoles by the combination of these

two processes. In the framework of the "wobbling-in-cone model"[33] $C \cdot A$ can be expressed as:

$$C \cdot A = \left[\frac{1}{2}\cos(\vartheta_0)(1+\cos(\vartheta_0))\right]^2 \quad (12)$$

where ϑ_0 is the cone half-angle of dipolar oscillation. With the value of $C \cdot A = 0.856$ we obtain $\vartheta_0 \approx 18.5°$, i.e., the maximum angular range explored by the combined vibration and restricted dipolar reorientation would be of the order of 37°. On the other hand, the slow component of the relaxation function would correspond to a global motion that fully randomizes the dipolar orientation. The nature of this process will be discussed in the Sec. III B.

Now, concerning the decay of cross correlations, Fig. 3 shows that, in contrast to the behavior of $\varphi_{self}(t)$, $\varphi_{cross}(t)$ displays a single-step decay, which seems to approximately follow a single exponential. To better characterize this decay, we have fitted $\varphi_{cross}(t)$ by a phenomenological generalized Debye function: $A\exp[-(t/\tau)^{\gamma}]$; with γ a shape parameter that can be smaller or larger than one. The fitting curve is included in Fig. 3 as a dashed line. We can see that the description is rather good in the full-time range, delivering a value of γ of 1.2, i.e., the cross-contribution results to be slightly "compressed." We also obtain a characteristic time, τ_{cross}, of about 15 ps. We note that, obviously, the model function describing the total dielectric relaxation, $\varphi(t) = \langle \vec{M}(0)\vec{M}(t)\rangle / \langle |\vec{M}(0)|^2 \rangle$, would be the addition of the functions describing both, self- and cross-contributions, properly weighted (see Fig. 3). Accordingly, apart from the vibrational process, the relaxation times characterizing the total dipolar relaxation would be just those characterizing both, the self- and cross-contributions: τ_0; τ_{self}; and τ_{cross}. However, from the experimental point of view, the usual procedure is to determine a main characteristic time from the total dipolar relaxation, the Debye time, τ_D, from the condition $\omega_{max}\tau_D = 1$—where ω_{max} is the frequency corresponding to the maximum of $\varepsilon''(\omega)$ at a given temperature. Even though the Debye time is a phenomenological time without any particular meaning from a microscopic point of view, we have mimicked this procedure with the data of $\varepsilon''(\omega)$ obtained from the simulations and reported in Fig. 2(a). We obtain a value of $\tau_D = 10.5$ ps, slightly larger than the experimental values ($\tau_D \approx 8$–9 ps) (we remind the shift factor of 1.3 for the frequency scale of the simulations used in the comparison with the experimental data shown in Fig. 2). According to these results, τ_{cross} results to be of the order of τ_D ($\tau_{cross} \approx 1.4\tau_D$). Then, we can conclude that the experimental phenomenological time, τ_D, approximately marks the time-scale at which cross-correlations decay to zero. On the other hand, we note that the total and single dipole relaxation times that we obtained approximately follow the Madden-Kivelson relationship $\tau_D/\tau_{self} \approx G_k$ (assuming that the so-called dynamic coupling parameter is of the order of 1).[34]

At this point, it is important to note that in some cases, the experimental values of $\varepsilon''(\omega)$ and/or $\varepsilon'(\omega)$ are usually fitted in the relaxation range by the addition of two or three Debye processes (see, e.g., Refs. 3, 35, and 36). By this completely phenomenological procedure, it is usually found that the most intense Debye contribution indeed corresponds to the so-called Debye peak ($\tau_D \approx 8$–9 ps at ≈300 K). The other (one or two) contributions—with smaller amplitudes and relaxation times in the range 0.1–1 ps—give account for the high-frequency deviations of $\varepsilon''(\omega)$ from the main Debye peak. The problem is that this kind of procedure uses to deliver different relaxation times that cannot be related with any physical process, in particular, in the high-frequency range. For example, in a recent paper,[37] the authors, following this procedure, they have interpreted the process with relaxation time of about 1 ps at ambient temperature, as due to the single-dipole reorientation (self-contribution in our terminology). Then, they have used the value of 1 ps to calculate the ratio between collective and single-dipole relaxation times (τ_D/τ_{self}). In this way they reported very high values of this ratio (≈8 at 300 K) that they use to check theoretical approaches. Our simulation results do not support this kind of procedure and interpretation. We unambiguously calculate the single-dipole reorientation function ($\varphi_{self}(t)$) that shows a main reorientation process with a time scale of about 5 ps.

B. Scattering-like magnitudes

First of all, in order to get insight about the molecular displacements at the time scales of the dielectric processes, we have calculated the mean squared displacement of the center of mass (CM) of water molecules ($\langle r^2(t)\rangle_{CM}$). The results obtained are included in Fig. 5(a). As expected, the long-time regime of $\langle r^2(t)\rangle_{CM}$ is proportional to time ($\langle r^2(t)\rangle_{CM} = 6Dt$ with $D = 2.627 \times 10^{-9}$ m^2 s^{-1}) indicating a pure diffusive regime for water molecules (from NMR: $D = 2.405 \times 10^{-9}$ m^2 s^{-1}[38]) at that time scale. We note, however, that in previous MD-simulations—carried out with a smaller cubic cell (about 65 Å side) and a TIP3P model of water—we have shown that the Q-dependence of the incoherent relaxation times corresponding to the oxygen motions (CM of water molecules), and the

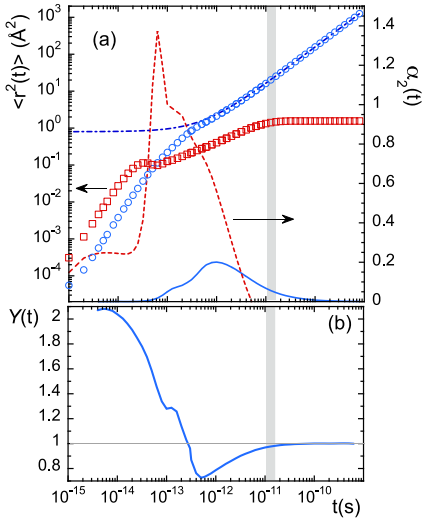

FIG. 5. (a) Mean squared displacement corresponding to the center of mass (CM) of water molecules (circles) and to the relative motion of hydrogen atoms (positive charges) of a water molecule with respect to the center of negative charges (M-point) (squares). The dashed-dotted line is the description (for $t > 1$ ps) of the mean squared displacement of the CM by the jump diffusion model (see the text). Non-Gaussian parameter, $\alpha_2(t)$, (continuous line) for the CM displacements and (dashed line) for the relative motion. (b) Effective power exponent $Y(t)$ for the CM motion (see the text). The thick gray line marks the time range τ_D–τ_{cross}.

corresponding $\langle r^2(t)\rangle_{CM}$, can be nicely described by a jump diffusion model with a jump diffusion time of about 0.3 ps and an average jump length of about 0.6 Å (see supplementary material of Ref. 7). The simulation data reported in this manuscript deliver similar results. Figure 5(a) includes the $\langle r^2(t)\rangle$ corresponding to a jump diffusion model: $\langle r^2(t)\rangle = 2\langle u^2\rangle + \ell^2 t/\tau_j$; where ℓ is the average jump length, τ_j the characteristic time and $\sqrt{\langle u^2\rangle}$ a measure of the dimension of the "thermal cloud." The curve included in the figure corresponds to $\sqrt{\langle u^2\rangle} = 0.63$Å; $\ell = 0.64$Å; and $\tau_j = 0.26$ ps. These values have been obtained by fitting (for $t > 1$ ps) the $\langle r^2(t)\rangle_{CM}$ calculated from the simulations. We see that the jump diffusion expression nicely describes the MD-simulation data for $t > 1$ ps. Obviously, the description fails in the short-time ballistic-like regime that in the framework of this model is represented by $\langle u^2\rangle$. We note that in the jump diffusion model, the pure diffusive regime characterized by $\langle r^2(t)\rangle_{CM} = 6Dt$ and $\alpha_2(t) = 0$, is only obtained at times rather long with respect to the jump time. In order to be more precise about when the water molecules reach this pure diffusive regime, we have represented in Fig. 5(b) the calculated function $Y(t)$ defined as $Y(t) = d[\log\langle r^2(t)\rangle_{CM}]/d[logt]$. We note that $Y = 2$ means pure ballistic displacement and $Y = 1$ pure diffusion. A minimum in $Y(t)$ would indicate some kind of restricted motions, being the depth of the minimum a measure of the "caging" strength. Figure 5(b) shows that water molecules reach a pure diffusive regime only at $t \sim \tau_D - \tau_{cross}$, i.e., at a time scale more than 30 times the jump time. It seems that the diffusion process of water molecules in general is rather homogeneous at molecular level as the non-Gaussian parameter indicates: $\alpha_2(t)$ is not very high in general (values smaller than 0.3 use to indicate almost Gaussian behavior[39]) and becomes zero (pure Gaussian, homogeneous behavior) once the isotropic diffusive regime is established. Thus, although the translation of water molecules clearly follows a jump-diffusion mechanism, at the time scale of τ_D–τ_{cross}, the behavior of the mean squared displacement and the non-Gaussian parameter—and thereby that of the self-part of the van Hove correlation function—cannot be distinguished from that corresponding to a pure continuous diffusion.

On the other hand, to obtain more information about the dynamics of the individual dipoles, we can follow the relative motion of the hydrogen atoms (positive electrostatic charges) of each water molecule with respect to the center of negative charges in the molecule (the so-called M-point in the geometry of water molecule used in the TIP4P-EW model[22]). First, we have calculated the mean squared displacement (MSD), $\langle r^2(t)\rangle$, corresponding to such a relative motion as well as the non-Gaussian parameter, $\alpha_2(t)$, which can be considered as a measure of the complexity and/or heterogeneity of the motions (see, e.g., Ref. 40). The results obtained are displayed in Fig. 5(a). As expected, the MSD of this relative motion increases with time until it reaches a constant value, which indicates a kind of "stable" (in time) localized relative motion of hydrogen atoms of each water molecule. We see that the time scale at which this constant value is reached is again of the order of τ_D–τ_{cross}. This is also the time scale at which the non-Gaussian parameter, $\alpha_2(t)$, of this relative motion—that was very high at short times—goes to zero. To know more about the type of localized motions involved, we can calculate the intermediate scattering function, $F_{HM}(Q,t)$, corresponding to this relative motion of H-atoms (see Sec. II C). Q is the momentum transfer. For a localized motion in general, $F(Q,t)$ can be expressed as:[41] $F(Q,t) = EISF(Q) + [1 - EISF(Q)]\emptyset(t)$, where $EISF$ is the elastic incoherent structure factor, which resembles the Fourier transformed asymptotic density distribution of moving atoms (H-atoms in our case). EISF in general depends on Q and this dependence informs us about the geometry of the localized motion.[41] This is the great advantage of $F(Q,t)$ function. On the other hand, $\emptyset(t)$ is a more or less complex function that depends on the problem we are considering. In any case, the localized nature of a motion implies that the characteristic time scale of $\emptyset(t)$ has to be constant for length scales larger than that of the localization. In other words, this time scale cannot depend on Q for Q values smaller than that associated to the localization length. The results obtained for $F_{HM}(Q,t)$ are shown in Fig. 6 for different Q-values in the range 0.3 to 5 Å^{-1}. The localized nature of the motions is clearly indicated by the long-time plateaus of $F_{HM}(Q,t)$, which define the $EISF(Q)$. The obtained values of $EISF(Q)$ in a wide Q-range, which extends until $Q = 10$ Å^{-1}, are shown in Fig. 7. The line through the points corresponds to the fitting with the function: $EISF(Q) = |\sin(QR)/QR|^2$, which is the mathematical model associated to an isotropic rotation on a spherical surface of radius R.[41] For the radius we obtain $R = 0.88$Å, which agrees rather well with the H-M average length of the water model used in the simulations.[22] Figure 6 shows that τ_D–τ_{cross} marks the time scale at which the long-time plateaus defining the EISF are established. Figure 6 also shows that the decay function $\emptyset(t)$ is rather complex and involves a first short-time decay—likely related to vibrational motions of the hydrogen atoms—and a second decay towards the final plateau that again cannot be described only by a single exponential function. As expected, $\emptyset(t)$, calculated as $\emptyset(t) = [F_{HM}(Q,t) - EISF(Q)]/[1 - EISF(Q)]$, does not depend on Q in the low-Q limit: $Q \lesssim 0.9$ Å^{-1}. Moreover, Fig. 3 shows that, properly scaled, $\emptyset(t)$ agrees rather well with the self-contribution function to the dipolar relaxation, $\varphi_{self}(t)$, calculated in an independent way. This indicates that the calculated scattering function in fact corresponds to the orientational

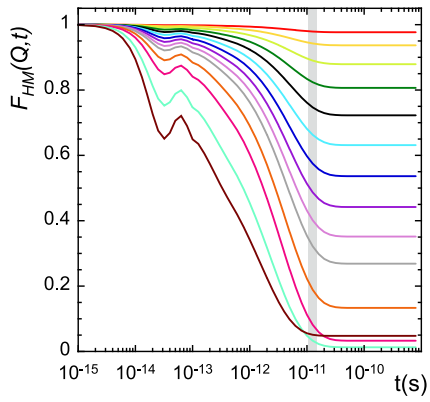

FIG. 6. Intermediate scattering function corresponding to the relative motion of hydrogen atoms (positive charges) of a water molecule with respect to the center of negative charges (M-point) for different Q (momentum transfer) values, from the top: 0.3; 0.5; 0.7; 0.9; 1.1; 1.3; 1.5; 1.7; 1.9; 2.1; 2.5; 3; 4; and 5 Å^{-1}. The thick gray line marks the time range τ_D–τ_{cross}.

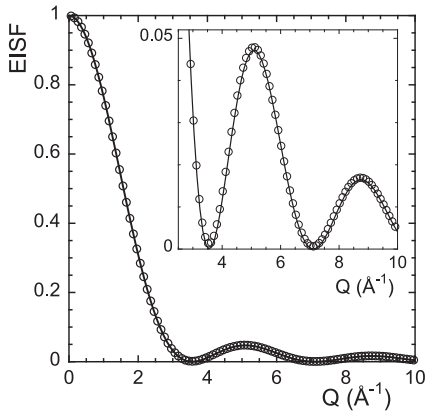

FIG. 7. Elastic incoherent structure factor [*EISF*(*Q*)] for the relative motion of hydrogen atoms (positive charges) of a water molecule with respect to the center of negative charges (M-point) (circles). The continuous line corresponds to the fitting curve $EISF(Q) = |\sin(QR)/QR|^2$ with R = 0.8825 Å. The inset shows a magnification of *EISF*(*Q*) in the reduced *Q*-range indicated.

correlation function of order one (Sears expansion terminology[42]), which is that describing the self-contribution of the dielectric relaxation. Moreover, the slow decay of $\emptyset(t)$ towards the plateau should be identified with the slow component of the relaxation function $[A\exp(-t/\tau_{self})]$ [Eq. (11)] that was introduced in the Sec. III A. What can we learn about this process from the EISF obtained? The problem is that the same EISF can be obtained for a model of continuous diffusion and for a model of isotropic rotational jumps. As in the case of translational diffusion (jump diffusion) discussed above, it has been shown by computer simulations that the rotation of water molecules take place by large angular jumps, which have been related to the breaking and reforming of hydrogen bonds and/or hydrogen bond exchange[32,43,44] in the framework of the Ivanov model.[45] Our results indicate, first of all, that the assumption of isotropy of these processes is a good approximation. We note that the process involving large angular displacements has to be rather complex at molecular level as the high values of the non-Gaussian parameter, $\alpha_2(t)$, indicate [see Fig. 5(a)]. However, at the time scale of τ_D–τ_{cross} the non-Gaussian parameter goes to cero and, according to the EISF, the reorientation of water molecules cannot be distinguished from a rotational diffusion. This is a similar situation to that found for molecular translation (see above). In fact, our results are in this way in line of those recently reported[46] that found that rotational dynamics of water molecules can be described as a Lévy rotor (non-Brownian) at intermediate times, due to hydrogen bond breaking and reforming, before becoming indistinguishable from Brownian dynamics at $t \sim 25$ ps.

IV. SUMMARY AND CONCLUSIONS

In conclusion, by comparing dielectric and scattering dynamic magnitudes that in some cases cannot be obtained experimentally, we have shown that: (i) the dipole-dipole correlations mediated by HBs are of paramount importance for the dielectric relaxation of water. They amount for almost a 60% of the total dielectric amplitude; (ii) these correlations decay at $t \sim \tau_{cross}$, which is of the order of the phenomenological time known as Debye time, τ_D; (iii) the correlation function corresponding to the cross-dipolar contribution is almost Debye-like and does not show any evidence of librations or fast processes; (iv) in contrast, the correlation function corresponding to the self-dipolar contribution is a two-step function. The first decay corresponds to dipolar librations. The second one to a dipolar relaxation process that is not unimodal. It can be described by a low-amplitude fast process (τ_0 = 0.31 ps) and a main slow process (τ_{self} = 5.4 ps) that fully randomizes the dipolar orientation; (v) then, the so-called Debye time has not any microscopic physical meaning. From a microscopic point of view, the times characterizing the dipolar relaxation of water are —apart from the libration processes—τ_0 = 0.31 ps, τ_{self} = 5.4 ps, and τ_{cross} = 15 ps. We note that these values do correspond to the MD-simulations carried out with the TIP4P-EW model of water. We could estimate the values for actual water by means of the shift factor (≈1.3) mentioned in the caption of Fig. 2. By applying this shift factor we would obtain: $\tau_0 \approx 0.24$ ps, $\tau_{self} \approx 4.15$ ps, and $\tau_{cross} \approx 11.5$ ps; (vi) although the translation and rotation of water molecules are "jump" processes in the short time range, at the time scale of about τ_D the observed behavior cannot be distinguished from that corresponding to uncoupled Brownian translational and rotational diffusion. These are the reasons why—even though the utmost importance of dipole–dipole correlations—the Debye model (that does not consider intermolecular dipolar interactions) seems to work at $t \gtrsim \tau_D$.

These results not only contribute to clarify a long-standing question but also open new views to general questions beyond water dynamics. In particular, the importance of cross correlations for the interpretation of dipolar relaxation in liquids and glass-forming systems and their relationships with the so-called Debye peak present in many different systems other than water.

ACKNOWLEDGMENTS

We acknowledge the Grant No. PID2021-123438NB-I00 funded by MCIN/AEI/10.13039/501100011033 and by "ERDF A way of making Europe," Grant No. TED2021-130107A-I00 funded by MCIN/AEI/10.13039/501100011033 and Unión Europea "NextGenerationEU/PRTR," as well as financial support of Eusko Jaurlaritza, code: IT1566-22 and from the IKUR Strategy under the collaboration agreement between Ikerbasque Foundation and the Materials Physics Center on behalf of the Department of Education of the Basque Government.

AUTHOR DECLARATIONS

Conflict of Interest

The authors have no conflicts to disclose.

Author Contributions

Fernando Alvarez: Data curation (equal); Formal analysis (equal); Software (equal); Writing – review & editing (equal). **Arantxa Arbe**: Conceptualization (equal); Funding acquisition (equal); Writing –

review & editing (supporting). **Juan Colmenero**: Conceptualization (equal); Data curation (equal); Formal analysis (equal); Methodology (equal); Writing – original draft (equal); Writing – review & editing (equal).

DATA AVAILABILITY

The data that support the findings of this study are available from the corresponding author upon reasonable request.

REFERENCES

[1] W. J. Ellison, K. Lamkaouchi, and J. M. Moreau, J. Mol. Liq. **68**, 171 (1996).
[2] P. J. W. Debye, *Polar Molecules* (Chemical Catalog Company, Incorporated, New York, 1929), pp. 77–108.
[3] N. Q. Vinh, M. S. Sherwin, S. J. Allen, D. K. George, A. J. Rahmani, and K. W. Plaxco, J. Chem. Phys. **142**, 164502 (2015).
[4] C. Ronne, L. Thrane, P. O. Åstrand, A. Wallqvist, K. V. Mikkelsen, and S. R. Keiding, J. Chem. Phys. **107**, 5319 (1997).
[5] N. Agmon, J. Phys. Chem. **100**, 1072 (1996).
[6] D. Bertolini, M. Cassettari, and G. Salvetti, J. Chem. Phys. **76**, 3285 (1982).
[7] A. Arbe, P. Malo de Molina, F. Alvarez, B. Frick, and J. Colmenero, Phys. Rev. Lett. **117**, 185501 (2016).
[8] D. C. Elton, Phys. Chem. Chem. Phys. **19**, 18739 (2017).
[9] A. Arbe, G. J. Nilsen, J. R. Stewart, F. Alvarez, V. G. Sakai, and J. Colmenero, Phys. Rev. Res. **2**, 022015(R) (2020).
[10] F. Alvarez, A. Arbe, and J. Colmenero, J. Chem. Phys. **155**, 244509 (2021).
[11] K. Koperwas and M. Paluch, Phys. Rev. Lett. **129**, 025501 (2022).
[12] D. Kivelson and P. Madden, Mol. Phys. **30**, 1749 (1975).
[13] C. J. F. Böttcher and P. Bordewijk, *Theory of Electrical Polarization*, 2nd ed. (Elsevier, Amsterdam, 1978).
[14] G. Williams, "Molecular aspects of multiple dielectric relaxation processes in solid polymers," in *Electric Phenomena in Polymer Science*, Advances in Polymer Science, Vol. 33 (Springer, Berlin, Heidelberg, 1979).
[15] T. Fukasawa, T. Sato, J. Watanabe, Y. Hama, W. Kunz, and R. Buchner, Phys. Rev. Lett. **95**, 197802 (2005).
[16] J. S. Hansen, A. Kisliuk, A. P. Sokolov, and C. Gainaru, Phys. Rev. Lett. **116**, 237601 (2016).
[17] F. Pabst, A. Helbling, J. Gabriel, P. Weigl, and T. Blochowicz, Phys. Rev. E **102**, 010606(R) (2020).
[18] J. P. Gabriel, P. Zourchang, F. Pabst, A. Helbling, P. Weigl, T. Böhmer, and T. Blochowicz, Phys. Chem. Chem. Phys. **22**, 11644 (2020).
[19] S. Carlson, F. N. Brünig, P. Loche, D. J. Bonthuis, and R. R. Netz, J. Phys. Chem. A **124**, 5599 (2020).
[20] C. Hölzl, H. Forbert, and D. Marx, Phys. Chem. Chem. Phys. **23**, 20875 (2021).
[21] P.-M. Déjardin, S. V. Titov, and Y. Cornaton, Phys. Rev. B **99**, 024304 (2019).
[22] H. W. Horn, W. C. Swope, J. W. Pitera, J. D. Madura, T. J. Dick, G. L. Hura, and T. Head-Gordon, J. Chem. Phys. **120**, 9665 (2004).
[23] R. Fuentes-Azcatl and J. Alejandre, J. Phys. Chem. B **118**, 1263 (2014).
[24] S. Blazquez, M. M. Conde, J. L. F. Abascal, and C. Vega, J. Chem. Phys. **156**, 044505 (2022).
[25] H. Yada, M. Nagai, and K. Tanaka, Chem. Phys. Lett. **464**, 166 (2008).
[26] P. Lunkenheimer, S. Emmert, R. Gulich, M. Köhler, M. Wolf, M. Schwab, and A. Loidl, Phys. Rev. E **96**, 062607 (2017).
[27] F. Alvarez, A. Alegra, and J. Colmenero, Phys. Rev. B **44**, 7306 (1991).
[28] G. L. Squires, *Introduction to the Theory of Thermal Neutron Scattering* (Dover, New York, 1996).
[29] T. Springer, *Quasielastic Neutron Scattering for the Investigation of Diffusive Motions in Solids and Liquids*, *Springer Tracts in Modern Physics* (Springer-Verlag, Berlin, 1972), Vol. 64.
[30] A. Rahman, K. S. Singwi, and A. Sjölander, Phys. Rev. **126**, 986 (1962).
[31] C. Zhang, J. Hutter, and M. Sprik, J. Phys. Chem. Lett. **7**, 2696 (2016).
[32] J. Qvist, C. Mattea, E. P. Sunde, and B. Halle, J. Chem. Phys. **136**, 204505 (2012).
[33] K. Kinosita, Jr., S. Kawato, and A. Ikegami, Biophys. J. **20**, 289 (1977).
[34] P. Madden and D. Kivelson, "A consistent molecular treatment of dielectric phenomena," in *Advances in Chemical Physics*, Vol. 56 (John Wiley & Sons, Inc., 1984), p. 467.
[35] R. Butchner, J. Barthel, and J. Stauber, Chem. Phys. Lett. **306**, 57 (1999).
[36] C. Ronne and S. R. Keiding, J. Mol. Liq. **101**, 199 (2002).
[37] N. Q. Vinh, L. C. Doan, N. L. H. Hoang, J. R. Cui, and B. Sindle, J. Chem. Phys. **158**, 204507 (2023).
[38] J. Qvist, H. Schober, and B. Halle, J. Chem. Phys. **134**, 144508 (2011).
[39] A. Narros, F. Alvarez, A. Arbe, J. Colmenero, D. Richter, and B. Farago, J. Chem. Phys. **121**, 3282 (2004).
[40] R. Zorn, Phys. Rev. B **55**, 6249 (1997).
[41] M. Bée, *Quasielastic Neutron Scattering* (IOP Publishing Ltd., Bristol, England, 1988).
[42] V. F. Sears, Can. J. Phys. **45**, 237 (1967).
[43] D. Laage and J. T. Hynes, Science **311**, 832 (2006).
[44] D. Laage and J. T. Hynes, J. Phys. Chem. B **112**, 14230 (2008).
[45] E. N. Ivanov, Sov. Phys. JETP **18**, 1041 (1964).
[46] D. A. Faux, A. A. Rahaman, and P. J. McDonald, Phys. Rev. Lett. **127**, 256001 (2021).